International Journal of Chemical Engineering and Applications, Vol. 1, No. 1, June 2010
ISSN: 2010-0221

Model Treatment for Simulation of Natural Convection in A vertical Wall Immersed In a Supercritical Fluid

Fayadh M. Abed and Dr. Ghazi Y. M. Alshahery

***Abstract*-An attempt for both Petal-Tejel and Van-der val EOS calculation of thermo physical properties; below, near and above psedo-critical line of supercritical flow of carbon dioxide. A good match of benchmark data with the calculation presented for thermal expansivity, heat conductivity, viscosity, specific heat and density. The flow characteristic being calculated to give a proper criterion with the physical meaning of flow at near psedo-ctritical temperature and pressure. The local Nusselt number was calculated and plotted as a function of the local Rayleigh number. It is observed in these plots that a curve obtained with temperature and pressure far from the critical region approaches the line obtained with a classic correlation. It was also observed that the curves corresponding to supercritical conditions are notably above of the line corresponding to the classic correlation, which means that the heat transfer considerably increases in the critical region. Nusselt-Rayleigh numbers ratios confirm the results of flow characteristics.**

***Index Terms:* Cubic equations of state, Natural convection, Supercritical carbon dioxide**

Nomenclature

a Equation of sate constant that corrects for intermolecular attractive forces $\left(N.m^4 / mol^2\right)$

b Equation of sate constant that corrects for intermolecular attractive forces ($\left(m^3 / mol\right)$

c Equation of sate constant

cp Specific heat (J/K-kg)

Gr Grashof Number

G Acceleration due to gravity

H Heat transfer coefficient $\left(W / m^2.k\right)$

M Molecule weight [g/mol]

Nu Nusselt number

P Pressure, bar

P_c Critical Pressure, bar

Pr Prandtl number

Ra Rayleigh number

Re Reynolds number

T Temperature (°C or K)

T_c Critical Temperature [K]

u Velocity in the vertical (*x*) direction

v Velocity in the horizontal (*y*) direction

x Distance in the vertical direction measured from the bottom of the plate

y Distance in the horizontal direction measured from the surface of the plate

U Dimensionless velocities in *x* directions

V Dimensionless velocities in *y* directions

Z Compressibility factor

Zc Critical Compressibility factor

Greek symbols

μ Dynamic viscosity (kg/m-s)

ρ Density (kg/m^3)

η *D*ynamic viscosity [pa.s]

ξ Inverse viscosity $\left[\mu P\right]^{-1}$

ω A centric factor 0.225 for CO_2

$\Omega_a, \Omega_b, \Omega_c$ Parameters in the a,b,c constants of EOS

β Volume coefficient of expansion for the fluid (= 1/*T* for an ideal gas)

γ Kinematics viscosity

α Thermal diffusivity [m^2/s]

λ Supercritical thermal conductivity

λ^0 Thermal conductivity at low pressure

Subscripts

Pc pseudocritical

W wall

f fluid

s surface

r reduced

∞ Free stream flow

c Critical property

i,j Index in x and y direction

Paper ID A501

N,M Number of grid point in x and y direction respectively

Abbreviation:

EoS Equation of state

SCF :Supercritical Fluid

NONDIMENSIONAL GROUPS

Nu Nusselt number [hL/ k]

$$Gr_L = \frac{g\beta(T_w - T_\infty)L^3}{\nu^2} \approx \frac{\text{Bouyancy force}}{\text{Viscous force}}$$

Fayadh M. Abed, Mechanical Engineering, College of Engineering, Tikrit University,
Corresponding Author (email: fayadh_mohamed@yahoo.com,Tel:00964(0)7702597719)
Dr. Ghazi Y. M. Alshahery, Former Director of the Iraq-Nuclear Program(00964(0)7701708838)

$$Ra_L = Gr_L \Pr = \frac{g\beta(T_w - T_\infty)L^3}{\nu\alpha}$$

I. Introduction

A supercritical fluid (SCF) is any substance at a temperature and pressure above its thermodynamic critical point. It has the unique ability to diffuse through solids like a gas, and dissolve materials like a liquid. Additionally, it can readily change in density upon minor changes in temperature or pressure. The specific behaviour of the supercritical fluids is of particular interest both from the theoretical point of view and for many industrial applications, such as the production of nanoparticles for medical use and the extraction of chemical compounds. SCF were first discovered in 1822 by Baron Gagniard de la Tour in his cannon ball experiments [1]. The importance of the heat transfer characteristics of supercritical fluids has been increased because of thermal dynamic behavior is quite different from subcritical. One of the most important characteristics of supercritical fluids near the critical point is that their physical properties exhibit rapid variations with the change of temperature, especially near the pseudocritical point (the temperature at which the specific heat reaches a peak for a given pressure) [2]. Highly charged machine elements such as gas turbine blades, supercomputer elements, magnets and power transmission cables are cooled with supercritical fluids[3]. Supercritical carbon dioxide is being used increasingly in industrial applications as an alternative to traditional organic, halogenated, and aqueous solvents [4], [5]. Ostrach (1952)[6] was one of the first to solve the boundary layer equations for natural convection from vertical flat plate using a numerical method, reducing the set of three equations (continuity, momentum and energy) to only two equations with their respective boundary conditions. He found that this type of flow is dependent on the Grashof number and Prandtl number. Sparrow and Gregg (1958)[7] gave a solution of this system in the case of exponential and power law temperature distributions. They showed the influence of the wall temperature distribution on heat transfer but they did not find a simple mathematical relation to express it. Nishikawa and Ito (1969)[8] did modeling for free convection to supercritical fluids based on boundary-layer equations and similarity transformation taking into account variable physical properties of the fluid. However, no effect of the temperature on the thermal expansivity was accounted for. Yang et al. (1972)[9] found a new similarity solution of the boundary-layer equations for more complicated wall temperature distributions. Their conclusions were similar to those of Sparrow and Gregg which confirmed that heat transfer is greatly affected by the wall temperature distribution. They showed that the local temperature difference between the wall and the medium is not sufficient to determine the local heat flux. McHugh and Krukonis (1994)[10] gave an excellent introduction to the properties and uses of supercritical fluids. Another alternative to study natural convection over a flat plate with an arbitrary temperature distribution is the use of numerical methods which are the most versatile for handling general boundary conditions (Merkin et al. 1996)[11]. Havet and Baly (1999)[12] have studied the turbulent natural convection over a vertical flat plate with finite-volume method. They also showed that buoyancy forces are locally affected by slope of temperature profile and heat transfer is greatly influenced by the wall temperature distribution. Supercritical fluids, particularly supercritical CO_2, have been used in areas ranging from materials cleaning, natural products extraction, chemical reactions, sample preparation and environmental remediation (Arai et al. 2001)[13]. The heat transfer by natural convection applied to simple geometries such as flat plates, spheres and cylinders have been extensively studied for decades. Information on many topics related to supercritical fluids applications is also abundant.

The supercritical fluid usually related to the presence of high temperature and pressure extreme as shown in Fig.1, the EOS at this conditions the fluid is not ideal, a requirement of a good representation of this fluid characteristic can be best fit to these characteristic by a model satisfy the property of continuity of critical isotherm at the critical point.

The objective of the present work is to determine the influence of EOS (Patel-Teja Model) on heat transfer by laminar natural convection over a vertical flat plate with a constant wall temperature into a supercritical fluid.

II. Theory

For the laminar vertical plate case a need for the laminar boundary layer equations to be incorporated with natural convection which is based on the assumptions of a steady, incompressible, two dimensional flow, with constant fluid properties and the Boussinesq approximation. In addition it is commonly assumed, that the velocity normal to the boundary is small, and derivations in direction of the flow are negligible.

Natural convection is observed when density gradients are present in a fluid acted upon by a gravitational field. Flow and heat transfer are analyzed by using the continuity, momentum and energy balance equations that govern these processes.

Free convection refers to fluid motion induced by buoyancy forces. The Buoyancy forces may arise in a fluid for which there are density gradients, and a body force that is proportional to density. In heat transfer, density gradients are due to temperature gradients and the body force is gravitational. The modeling of this case can be best described as shown in Figure.2 the governing equations to satisfy this model are as follow:

$$\frac{\partial u}{\partial x} + \frac{\partial v}{\partial y} = 0 \qquad \text{Continuty (1)}$$

$$u\frac{\partial u}{\partial x} + v\frac{\partial u}{\partial y} = \beta g(T - T_\infty) + \nu\frac{\partial^2 u}{\partial y^2} \qquad \text{Momentum (2)}$$

$$u\frac{\partial T}{\partial x} + v\frac{\partial T}{\partial y} = \alpha\frac{\partial^2 T}{\partial y^2} \qquad \text{Energy (3)}$$

To handle the above equation into a numerical methods

of calculations, it is convenience to convert the governing equation to dimensionless formula as follow:

$$\frac{\partial U}{\partial X}+\frac{\partial V}{\partial Y}=0 \qquad \text{Continutiy (4)}$$

$$U\frac{\partial U}{\partial X}+V\frac{\partial U}{\partial Y}=\theta\beta^{*}+\frac{\partial^{2}U}{\partial Y^{2}} \qquad \text{Momentum (5)}$$

$$U\frac{\partial \theta}{\partial X}+V\frac{\partial \theta}{\partial Y}=\frac{1}{\Pr}\frac{\partial^{2}\theta}{\partial Y^{2}} \qquad \text{Energy (6)}$$

Where

$$X=\frac{x}{LG^{0}},\ Y=\frac{y}{W},\theta=\frac{T-T_{\infty}}{T_{s}-T_{\infty}}$$

$$U=\frac{uW^{2}}{\nu LG^{0}},\ V=\frac{vW}{\nu},\ G^{0}=\frac{\beta_{ref}g(T_{s}-T_{\infty})W^{4}}{\nu^{2}L}$$

$$\beta_{ref}=1/T_{f},\ T_{f}=\tfrac{1}{2}(T_{s}+T_{f}),\ \beta^{*}=\beta/\beta_{ref}$$

$$\left.\begin{aligned}
&\left.\frac{\partial U}{\partial Y}\right|_{i,j}=\frac{U_{i,j+1}-U_{i,j}}{2\Delta Y},\ \left.\frac{\partial^{2}U}{\partial^{2}Y}\right|_{i,j}=\frac{U_{i,j+1}-2U_{i,j}+U_{i,j-1}}{\Delta Y^{2}},\\
&\left.\frac{\partial U}{\partial X}\right|_{i,j}=\frac{U_{i,,j}-U_{i-1,j}}{\Delta X},\\
&\left.U\frac{\partial U}{\partial X}\right|_{i,j}\cong U_{i-1,j}\left(\frac{U_{i,,j}-U_{i-1,j}}{\Delta X}\right),\\
&\left.V\frac{\partial U}{\partial Y}\right|_{i,j}\cong V_{i-1,j}\left(\frac{U_{i,,j+1}-U_{i,j-1}}{2\Delta Y}\right)
\end{aligned}\right\} \qquad (7)$$

by substitution equation (7) into momentum Eq.5 and rearrangement yield:

$$\left(-\frac{V_{i-1,j}}{2\Delta Y}-\frac{1}{\Delta Y^{2}}\right)U_{i,j-1}+\left(\frac{U_{i-1,j}}{\Delta X}-\frac{2}{\Delta Y^{2}}\right)U_{i,j}+\left(\frac{V_{i-1,j}}{2\Delta Y}-\frac{1}{\Delta Y^{2}}\right)U_{i,j+1}=\theta_{i-1,j}\beta^{*}+\frac{U^{2}{}_{i-1,j}}{\Delta X}$$

$$C_{j}U_{i,j-1}+D_{j}U_{i,j}+E_{j}U_{i,j+1}=F_{j} \qquad (8)$$

are coefficients C_{j},D_{j},E_{j} and F_{j} where;

Equation (8) gives a set of N-2 equations and N-2 unknown values of U, i.e., $U_{i,2},U_{i,3},U_{i,4},\ldots\ldots\ U_{i,N-2},U_{i,N-1,}$ along the i-the line to each of the points j=2,3,4,..N-1.

$U_{i1,},U_{i,N}=0$ (Momentum equation boundary condition).then the energy equation (6) the substitution as follow:

$$\left.\begin{aligned}
&\left.U\frac{\partial\theta}{\partial X}\right|_{i,j}\cong U_{i-1,j}\left(\frac{\theta_{i,j}-\theta_{i-1,j}}{\Delta X}\right),\\
&\left.V\frac{\partial\theta}{\partial Y}\right|_{i,j}\cong V_{i-1,j}\left(\frac{\theta_{i,,j+1}-\theta_{i,j-1}}{2\Delta Y}\right),\\
&\left.\frac{\partial^{2}\theta}{\partial Y^{2}}\right|_{i,j}\cong\frac{\theta_{i,j+1}-2\theta_{i,j}+\theta_{i,j-1}}{\Delta Y^{2}}
\end{aligned}\right\} \qquad (9)$$

By substitution equation (9) into the energy equation (6) and rearranging yield:

$$\left.\begin{aligned}
&\left(-\frac{V_{i-1,j}}{2\Delta Y}-\frac{1}{\Pr\Delta Y^{2}}\right)\theta_{i-1,j}+\left(\frac{U_{i-1,j}}{\Delta X}-\frac{2}{\Pr\Delta Y^{2}}\right)\theta_{i,j}\\
&+\left(\frac{V_{i-1,j}}{2\Delta Y}-\frac{1}{\Delta Y^{2}}\right)\theta_{i,j+1}=\frac{U_{i-1,j}\theta_{i-1,j}}{\Delta X}
\end{aligned}\right\} \qquad (10)$$

The general form of equation 10 has the following form

$$G_{j}\theta_{i,j-1}+H_{j}\theta_{i,j}+S_{j}\theta_{i,j+1}=J_{j} \qquad (11)$$

Equation (11) gives a set of N-2 equations and N-2 unknown values of U, i.e., $\theta_{i,2},\theta_{i,3},\theta_{i,4},\ldots\ldots\ \theta_{i,N-2},\theta_{i,N-1,}$ along the i-the line to each of the points j=2,3,4,..N-1.

$\theta_{i,1}=1,\quad \theta_{i,N=0}$ energy equation boundary conditions. The system of Eq. 8 and 11 is a tridiagonal matrix and solved by Thomas algorithm[15], which are needed a continuity requirement. The continuity requirement equation is desctitized as shown in Fig. 3 The derivatives are descritized at the midpoint. Applying the central-difference approximation in Y-direction in the following:

$$\left.\frac{\partial V}{\partial Y}\right|_{i,j-1/2}=\frac{V_{i,,j}-V_{i,j-1}}{\Delta Y} \qquad (12)$$

Where X-derivative at the point(i,j-1/2) is equal to the average of the X-derivative at the point (i,j) and (i,j-1).

Then

$$\left.\frac{\partial U}{\partial X}\right|_{i,j-1/2}\cong\frac{1}{2}\left[\left.\frac{\partial U}{\partial X}\right|_{i,j}+\left.\frac{\partial U}{\partial X}\right|_{i,j-1}\right] \qquad (13)$$

The following finite difference approximation for the continuity equation is obtained by Substituting Eqs. 12 and 13 into $\frac{\partial V}{\partial Y}=-\frac{\partial U}{\partial X}$ which yield

$$\frac{V_{i,j}-V_{i,j-1}}{\Delta Y}=-\frac{1}{2}\left(\frac{U_{i,j}-U_{i-1,j}}{\Delta X}+\frac{U_{i,j-1}-U_{i-1,j-1}}{\Delta X}\right)$$

Then

$$V_{i,j}=V_{i,j-1}-\left(\frac{\Delta Y}{2\Delta X}\right)\begin{pmatrix}U_{i,j}-U_{i-1,j}\\+U_{i,j-1}-U_{i-1.j-1}\end{pmatrix} \qquad (14)$$

Where the variables $U_{i,j},U_{i-1,j},U_{i,j-1},U_{i-1.j-1}$ is calculated from solving the system of momentum equations. This solution approached is shown in Fig.4.

III. Problem and Boundary Conditions

The geometry and the coordinate system of the present problem are shown in Figs. 2. The plate is immersed in a supercritical fluid which is assumed to be maintained at a

uniform temperature and the fluid movement is entirely driven by buoyancy forces. In this problem, the gravity acts in the negative x direction. The coordinate system is chosen such that x measures the distance along the plate and y measures the distance normal to it. Far away from the plate, the velocity and the temperature of the uniform main stream are U_∞ and T_∞ , respectively. Since the heated surface is stationary, the fluid velocity at the surface must be zero. Far from the surface, the velocity is also zero. In between, thermal and momentum boundary layers develop, where the velocity is non-zero. These begin at the bottom edge of the plate and become thicker with increasing distance up the plate.. The profiles of the temperature and the velocity components (v_x and v_y). The boundary conditions for the velocity and temperature fields are:

$$T = T_w \text{ at } y = 0,\ T = T_\infty \text{ for } y \to \infty,\ u = v = 0 \text{ at } y = 0,\ u = v = 0 \text{ for } y \to \infty$$

Conduction and viscous transport of momentum in the *x* direction are neglected. The velocity and temperature gradients are considered to obey the following relations:

$$\frac{\partial v}{\partial x} \rangle\rangle \frac{\partial v}{\partial y}, \frac{\partial u}{\partial x}, \frac{\partial u}{\partial y}, \text{ and } \frac{\partial T}{\partial x} \rangle\rangle \frac{\partial T}{\partial y},$$

IV. Supercritical Fluid Properties Estimation

In order to account for the non ideal gas behavior under critical and supercritical conditions, mainly, conductivity, viscosity, specific heat and thermal expansivity. Despite the difficulty to predict the behavior of supercritical fluid properties without a detail experimental and theoretical study. But by using Stiel and Thods methods [16], the supercritical fluid thermal conductivity is estimated accordingly having the following relation.

$$(\lambda - \lambda^0)\Gamma Z_c^5 = 1.22\, x10^{-2}\left[e^{(0.535\,\rho_r)} - 1\right],\ \rho_r \langle 0.5$$

$$(\lambda - \lambda^0)\Gamma Z_c^5 = 1.14\, x10^{-2}\left[e^{(0.67\,\rho_r)} - 1.069\right],\ 0.5 \langle \rho_r \langle 2.0$$

$$(\lambda - \lambda^0)\Gamma Z_c^5 = 2.60\, x10^{-2}\left[e^{(1.155\,\rho_r)} + 2.016\right],\ 2.0 \langle \rho_r \langle 2.8$$

Where $\rho_r = \dfrac{3PT_C}{8ZP_cT_f}$ and $\Gamma = 210\left(\dfrac{T_c M^3}{P_c^4}\right)^{\frac{1}{6}}$,

$\lambda^0 = 18.006 * 10^{-3}\, w/m.k$ (For Carbon Dioxide)

Where λ^0 is the ideal-gas or low-pressure limit of the thermal conductivity and ρ_r is the reduced density. Further estimation of Viscosity, specific Heat and Density, A method of Reinchenberg methods[17] and Poling et al.[18] is recommended for dense fluids at super- or near-critical conditions having the following relation for the viscosity.

$$\mu = \mu_0\left(1 + Q_v \frac{A_v P_r^{3/2}}{B_v P_r + \left(1 + C_v P_r^{D_v}\right)^{-1}}\right)$$

$$A_v = \frac{\alpha_1}{T_r} e^{\alpha_2 T_r^\alpha},\ B_v = A_v(\beta_1 T_r - \beta_2)$$

$$C_v = \frac{\gamma_1}{T_r} e^{\gamma_2 T_r^c},\ D_v = \frac{\lambda_1}{T_r} e^{\lambda_2 T_r^d},\ Q_v = 1.0$$

$$\alpha_1 = 1.982510^{-03},\ \alpha_2 = 5.2683,\ \alpha = -0.5767$$

$$\beta_1 = 1.6552,\ \beta_2 1.2760,\ \gamma_1 = 0.1319,\ \gamma_2 = 3.7035$$

$$c = -79.8678,\ \lambda_1 = 2.9496,\ \lambda_2 = 2.9190,\ d = -16.6169$$

The results of thermal conductivity and Viscosity estimation are presented in Fig.5

Thermal conductivity decrease with increasing temperature. Its shows, however, a local maximum near the pseudo-critical point. Beyond the pseudo-critical temperature thermal conductivity decreases sharply. Similar behavior shows also dynamic viscosity. The heat capacities of real gases are related to the corresponding values in the ideal-gas or low-pressure state, (at the same temperature and composition) by the following definition: $C_p = C_p{}^0 + \Delta C_p$ where, ΔC_p is the so-called residual heat capacity which has the form $\Delta C_p = C_p - C_p{}^0 = (\Delta C_p)^0 + \omega(\Delta C_p)^1$ [14], However the heat capacity behavior can be understood with respect with reduce pressure and temperature as presented in Fig.6.

From this figure immediately one can note that there is a local maximum of the specific heat capacity at each pressure, while in the sub-critical range the maximum specific heat locates on the saturation line. At the critical point specific heat its maximum value.

V. Thermal Expansion Coefficient Estimation

In calculation it is important to use the cubic equations of state EOS derived from van der Waals EOS. Among the many cubic EOS nowadays available, those of Redlich and Kwong (1949)[19], Soave (1972)[20], Trebble, M.A. and Bishnoi, P.R. (1986) [21] and of Patel and Teja (1982)[22], All the EOS give higher deviations near the critical point, specially the two-parameter equations when it is considered, $\left(\partial P / \partial V\right)_T = 0, \left(\partial^2 P / \partial^2 V\right)_T = 0$. This fact is expected of any cubic equation which predicts a unique critical compressibility factor (*Z*c), to fulfill the property of continuity of the critical isotherm at the critical point. In the present work Patel-Teja EOS is used

$$P = \frac{RT}{(V-b)} - \frac{a}{V(V+d)+c(V-d)} \qquad (15)$$

In order to express Eq.15 in term of Compressibility factor (z), the following definitions are obtained in the form:

$$\left.\begin{array}{l} Z^3+Z^2(C+D-B-1)+ \\ (A-BD-BC-C-CD-D)Z \\ +(BCD-AB+CD)=0 \end{array}\right\} \quad (16)$$

The thermal expansivity as a function of pressure and temperature, is an implicit derivative of Eq. 16 with respect to Temperature at constant Pressure and given in the following form:

$$\left.\begin{array}{l} \left[3Z^2+2Z(C+D-B-1)+(A-BD-BC-C-CD-D)\right]\left(\frac{\partial Z}{\partial T}\right)_p \\ -Z^2\left(\left(\frac{\partial C}{\partial T}\right)_p+\left(\frac{\partial D}{\partial T}\right)_p-\left(\frac{\partial B}{\partial T}\right)_p\right)+ \\ Z\left(\begin{array}{l}\frac{\partial A}{\partial T}-B\left(\frac{\partial D}{\partial T}\right)_p-D\left(\frac{\partial B}{\partial T}\right)_p-\left(\frac{\partial C}{\partial T}\right)_P- \\ C\left(\frac{\partial D}{\partial T}\right)_p-D\left(\frac{\partial C}{\partial T}\right)_p-\left(\frac{\partial D}{\partial T}\right)_P\end{array}\right) \\ +\left(\begin{array}{l}BC\left(\frac{\partial D}{\partial T}\right)_P+D\left(\frac{\partial BC}{\partial T}\right)_P-A\left(\frac{\partial B}{\partial T}\right)_P-B\left(\frac{\partial A}{\partial T}\right)_P \\ +C\left(\frac{\partial D}{\partial T}\right)_P+D\left(\frac{\partial C}{\partial T}\right)_P\end{array}\right) \end{array}\right\} \quad (17)$$

Where $Z = PV/RT$, $A = aP/(RT)^2$, and $B = bP/RT$, $C = cP/RT$, and $D = dP/RT$ then

$$a=\Omega_a\left(\frac{R^2T_c^2}{P_c}\right)\left[1+F\left(1-\sqrt{T_r}\right)\right]^2 \quad , \quad b=\Omega_b\left(\frac{R^2T_c}{P_c}\right) \quad ,$$

$$c=\Omega_c\left(\frac{R^2T_c}{P_c}\right), \Omega_c=1-3\xi_c \text{, and}$$

$$\Omega_a=3\xi_c^2+3(1-2\xi_c)\Omega_b+\Omega_b^2+1-3\xi_c$$

Where Ω_b is the smallest positive root of the cubic equation:

$$\Omega_b^3+(2-3\xi_c)\Omega_b^2+3\xi_c^2\Omega_b-3\xi_c^3=0$$

F and ξ_c are functions of the a centric factor given by the following correlations:

$$F=0.452413+1.30982\omega-0.295937\omega^2,$$

$$\xi_C=0.329032-0.076799\omega+0.02119477\omega^2$$

Finally the thermal expansion compressibility β is a function of compressibility factor which obtained by substituting all the derivative results of the variable A,B,C and D into Eq. (17)

$$\beta=\frac{1}{T}\left[1-\left(\frac{\begin{array}{l}Z(-2A+2BD+2BC+2CD+C+D) \\ +(-3BCD+3AB-2CD)\end{array}}{\begin{array}{l}3Z^3+2Z^2(C+D-B-1)+ \\ Z(A-BD-BC-C-CD-D)\end{array}}\right)\right] \quad (18)$$

The calculation of β involves two steps; first, the compressibility factor, Z, is determined by finding the appropriate root of Eq. (16); then inserting into Eq. (18) the value of β is obtained. It is interesting to verify that Eq. (18) converges to $(1/T)$ at the ideal-gas limit. This limit is reached as $P\to 0$ at constant temperature $P\to 0$, $PV'\to RT$, i.e.,

i.e., $Z\to 1$ and $A\to 0$, $B\to 0$, $C\to 0$, $D\to 0$

Therefore, $\beta=1/T$.

These calculation with Patel-Teja model and ideal fluid and others being performed in the Figure. 7

VI. Convergence History:

For the solution of the three coupled equations, an iterative procedure was used with an under-relaxation coefficient of (0.15-0.2) for a quicker convergence of the temperatures and velocities. Under-relaxation is usually used when the equations are non-linear. In this case, the relaxation coefficient being used between 0 and 1. The quality of the mesh plays a significant role in the accuracy and stability of the numerical computation. This is attribute to the associated mesh quality and node distribution, smoothness and skewness. In the current study a clustering function was used which gives best distribution of grid point in the region of flow gradients, especially at the boundary layers region (Fig.8). Before carrying out the final calculations, grid dependency test and code validation studies were performed.

A grid optimization were used to finalized best results. The convergence criteria that is used for this work is velocity changes less than 1%.

VII. Results and Discussion

A thermodynamic model has been developed to represent the thermal expansivity of real fluids based on an equation-of-state approach. The approach depends on an estimation supercritical fluid properties at critical conditions, mainly conductivity, viscosity, specific heat, density and Thermal expansivity.

Thermal expansion coefficient results are presented based on Patel-Teja model and van der Waals (EOS). These values are presented graphically, where they are compared with the ideal-gas and reference values. The selected values of pressures 3.69 MPa , 7.38 MPa and 10 MPa. Being chosen for the calculation due to the existence of experimental benchmark data available for comparison Angus et al.[23] Fig.8. The calculated data and the experimental value represented show an excellent fit. Further more when a temperature increase beyond the critical region both ideal and real thermal expansively coincide in their behavior. This results convincingly attributed to the intermolecular forces is vanishing at higher temperature.

Specific heat and density values with respect to temperature at specific value of pressure are presented in Fig.9. The results show at the critical temperature both values of specific heat and density have a major changes with a peak value of specific heat and drop in density values at this point. This result is confirmed by the study of specific heat of CO_2 of YANG et. el.[9] at different

pressure. The results showed the same trends with regard to temperature with respective to the variation of specific heat and density. As far as the pressure change from 7.4 MPa to 7.5 MPa, however the small changes of pressure gives a miner shift in position of the physical property to a higher value.

The model presented in this calculation can be adequately predict the thermo physical properties below, at and above the pseudo characteristics. The critical point of a fluid is defined as the point at which a distinction between liquid and gaseous phases disappears [24]. Beyond the critical point, thermo physical properties of the fluid vary continuously with temperature [25]. While a supercritical fluid cannot correctly be defined as either a liquid or a gas, at points above the pseudo critical line the fluid behaves more like a liquid and at points below the pseudo critical line the fluid behavior more closely resembles a gas. The thermo physical properties of supercritical fluids change rapidly near the pseudo critical point. This introduces difficulty in predicting heat transfer and fluid flow performance. To elaborate this difficulty, due to the major changes taken place in the thermal physical properties noticeable in fig. 10. The velocity of the flow contour as shown in Fig. 10.a, b and c for below ,at and above the pseudo critical line. In Fig. 10.a which is below the critical line show a wedge shape which is stagnation like point between the gas and fluid, while in Fig.10.b the contour of the stagnant point appeared as a closed circle which may be a whirl type flow in a boiling fluid which is like gas bubbling in fluid. At Fig. 10.c the velocity contours appear as a wavy texture which is a liquid like flow.

The Nusslet number also enhance this result which peak up at the critical point. In the same way the heat transfer coefficient represent the higher values with gas CO_2 and lower values for liquid with the transition point at the critical point as shown in Fig.11

The calculations were achieved at reduced pressure of 1.05 with different critical reduced temperature 1.0, 1.05 and 1.1. and plotted in logarithmic scale so the curves approach straight lines. The figure shows some oscillations at critical point due to transition from sub critical to supercritical region. The results of numerical calculations of Nusslet number values are compared to the empirical correlation, and we concluded that at higher the temperature, the closer the lines to that representing the empirical correlation. Here the effect of the temperature on the local heat transfer coefficient can be seen. Consequently in comparison for empirical form of flow compared to Churchill and Chu [26] the flow is consistent linearly ratio of numbers Nusslet to Rayleigh with respect to different value of temperatures at constant and variable pressure as shown in Fig.12.a,b. the disembarking from linearity due gas fluid transition.

The figures show that the line of reduced pressure of 1.05 and 1.1 at almost superimposed. Fom this case, it can conclude that the effect of the pressure is not significant, while on the other condition when the reduced pressure at 0.2 the line become closer to empirical correlation line. The curve corresponds to the empirical correlation is obtained from relation that was proposed by Churchill and Chu (1975) and it is applicable over a wide range of Rayleigh numbers. This is:

$$N\overline{u}_L = 29.976\left(\frac{0.802+0.670RaL^{1/4}}{1.180}\right)$$

$$Ln\left(\frac{0.802+0.678RaL^{1/4}}{0.802+0.661RaL^{1/4}}\right) \quad 0 < \mathrm{Ra}_L < 10^9$$

Finally in all cases encountered Patel-Teja model give an excellent agreement with Van dar EOS.

VIII. Conclusion

In the present work it has being shown that the Patel model (EOS) giving reasonable approach in calculating the thermophysical properties of supercritical flow. However it is noticeable that the flow as well as the thermophysical properties has a varies considerably over a small changes in pressures and temperatures. This lead to a conclusion that the benefit of various properties to be a attained at the working conditions has to be controlled tightly.

Referrenecs

[1] www.science.fau.edu/chemistry/mdj/pchem/ Supercritical Fluids.pdf
[2] Liao SM, Zhao TS. 2002, Measurements of heat transfer coefficients from supercritical carbon dioxide flowing in horizontal mini/micro channels, *Transactions of the ASME Journal of Heat Transfer,* 124:413-420.
[3] Liao SM, Zhao TS. 2002,An experimental investigation of convection heat transferto supercritical carbon dioxide in miniature tubes, International Journal of Heat and Mass Transfer 45 (2002) 5025–5034
[4] Wells, S.L. and DeSimone. J., "CO_2 Technology Platform: An Important Tool for Environmental Problem Solving." Angew. Chem. Int. Ed., 2001. 40: pp. 518-527.
[5] DeSimone, J.M. and J.S. Keiper, "Surfactants and self-assembly in carbon dioxide. Current Opinion in Solid State and Materials Science." 2001. 5: pp. 333-341.
[6] Ostrach, S. 1952. An Analysis of Laminar Free-Convection Flow and Heat Transfer about a Flat Plate Parallel to the Direction of the Generating Body Force. Report 1111- Supersedes NACA TN 2635.
[7] Sparrow, M. & Gregg J.L. 1958. Similar solutions for free convection from a nonisothermal vertical plate. Transactions of the ASME 80:379-386.
[8] Nishikawa, K. & Ito, T. 1969. An analysis of Free-Convective Heat Transfer from an Isothermal Vertical plate to Supercritical fluid. International Journal of Heat Mass Transfer 12:1449-1463.
[9] Yang, K.T. & Novotny, J.L. & Cheng, Y.S. 1972. Laminar free convection from a nonisothermal vertical plate immersed in a temperature stratified medium. Transactions of the ASME 80:1097-1109.
[10] McHugh, M. A. & Krukonis, V. J. 1994. Supercritical Fluid Extraction: Principles and Practice, Butterworth, Heinemann.
[11] Merkin, J.H. & Pop, I. 1996. Conjugate free convection on a vertical surface. International Journal of Heat and Mass Transfer 39 (7): 1527-1534.
[12] Havet, M. & Blay, D. 1999. Natural convection over a non-isothermal vertical plate. Journal of Heat Transfer, 42:1410-1424.
[13] Arai, Y. & Sako, T. & Takebayashi, Y. 2001. Supercritical Fluids-Molecular Interactions, Physical Properties and New Applications. First Edition, Springer, Berlin, Germany.
[14] T. Clifford, "Fundamentals of Supercritical Fluids," Oxford University Press, New York, 1999.
[15] http://en.wikipedia.org/wiki/Tridiagonal_matrix_algorithm.
[16] Stiel, L.I., and Thodos, G., AICHE J., Vol. 10, pp. 26, 1964.
[17] Reichenberg, D., "The Viscosities of Gases at High Pressures," Natl. Eng. Lab.,
Rept. Chem. 38, East Kilbride, Glascow, Scotland, August 1975.

[18] Poling et al., "Properties of Gases and Liquids", 5th ed. McGraw-Hill, New York
[19] Redlich, O. and Kwong, J.N.S. (1949) On the Thermodynamics of Solutions. V. An Equation of State. Fugacities of Gaseous Solutions. Chem. Rev., 44, 2, 233-244.
[20] Soave, G. (1972) Equilibrium Constants from a Modified Redlich-Kwong Equation of State. *Chem. Eng. Sci.*, 27, 1197-1203.
[21] Trebble, M.A. and Bishnoi, P.R. (1986) Accuracy and Consistency Comparisons of Ten Cubic Equations of State for Polar and Non-Polar Compounds. *Fluid Phase Equil.*, 29, 465-474.
[22] Patel, N.C. and Teja, A.S. (1982) A New Cubic Equation of State for Fluids and Fluid Mixtures. *Chem. Eng. Sci.*, 37, 3, 463
[23] Angus, S. & Armstrong, B. & Reuck, K. 1976. International Thermodynamic Tables of the Fluid State-Carbon Dioxide. First Edition, Pergamon Press, Headington Hill Hall, Oxford OX3 0BW, England
[24] T. Clifford, "Fundamentals of Supercritical Fluids," Oxford University Press, New York, 1999.
[25] Song, H., "Investigation of a Printed Circuit Heat Exchanger for Supercritical CO2 and Water," M.S. Degree Thesis, Kansas State University, 2007.
[26] Churchill, S.W. and Chu, H.H.S., "Correlating Equations for Laminar and Turbulent Free Convection from a Horizontal Cylinder", International Journal of Heat and Mass Transfer, Vol. 18, 1975, pp. 1323-1329.

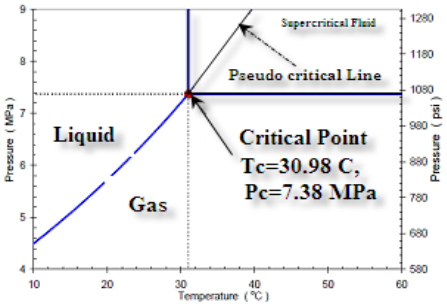

Fig.1 Phase diagram for carbon dioxide[14]

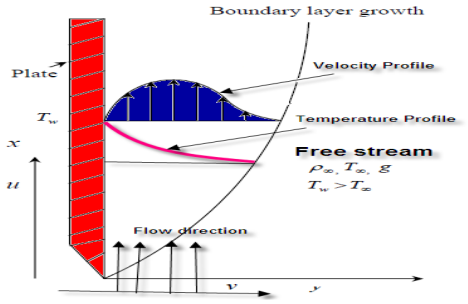

Fig.2 Heated Flat plate

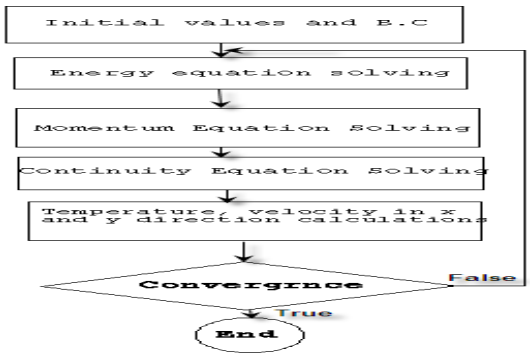

Fig. 4 Numerical Approach Flowchart

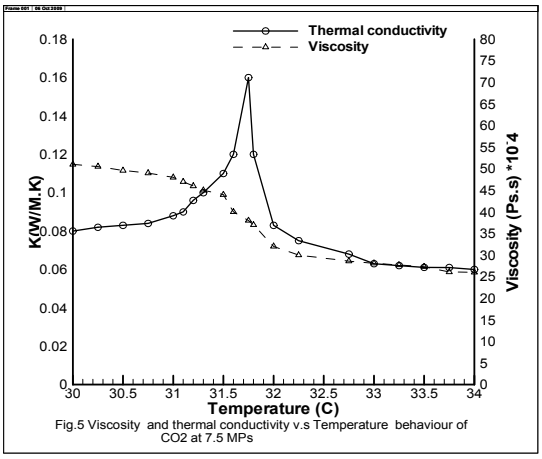

Fig.5 Viscosity and thermal conductivity v.s Temperature behaviour of CO2 at 7.5 MPs

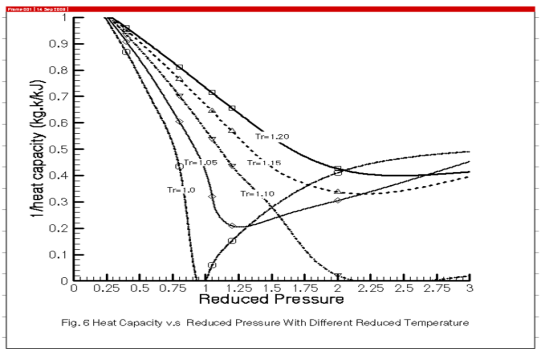

Fig. 6 Heat Capacity v.s Reduced Pressure With Different Reduced Temperature

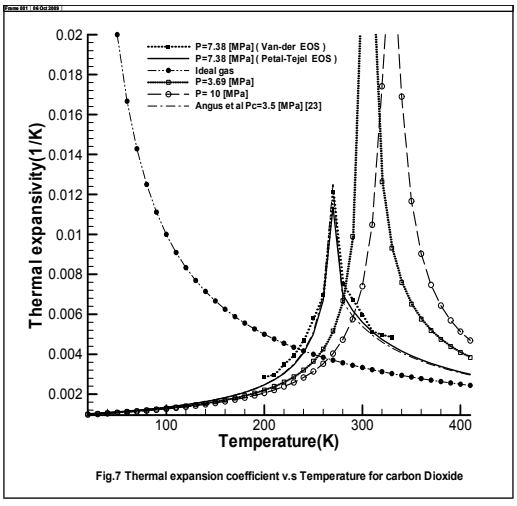

Fig.7 Thermal expansion coefficient v.s Temperature for carbon Dioxide

$$Clusterfunction = 1 - \Gamma * \frac{gg-1}{gg+1}, \text{where } gg = \left(\frac{\Gamma+1}{\Gamma-1}\right)^{\lambda}$$

Γ is ranging from $(1-\infty)$, $\lambda = 1-(\kappa-1)/(N-1)$, $1 \le \kappa \le N$, N number of Grid Point

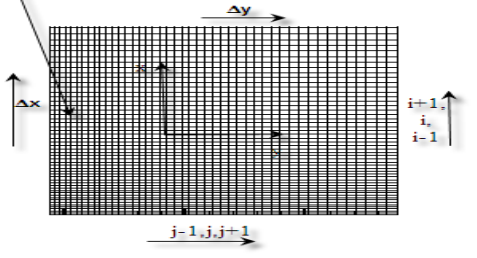

Fig 8 Flat Plate Mesh Distribution

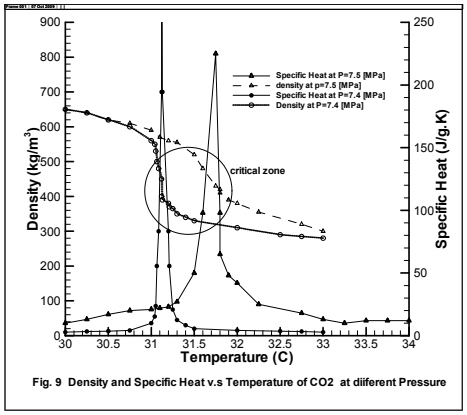

Fig. 9 Density and Specific Heat v.s Temperature of CO2 at diiferent Pressure

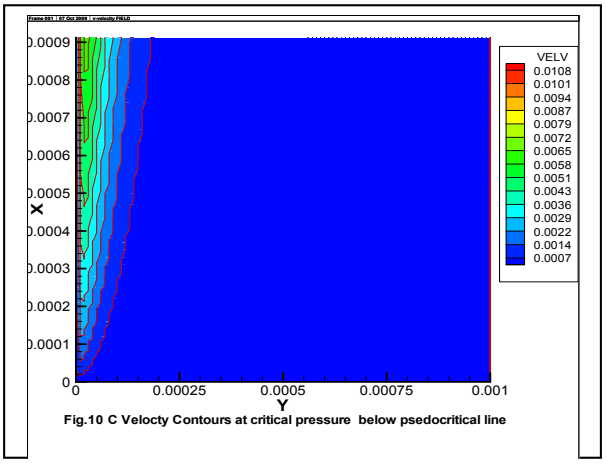

Fig.10 C Velocty Contours at critical pressure below psedocritical line

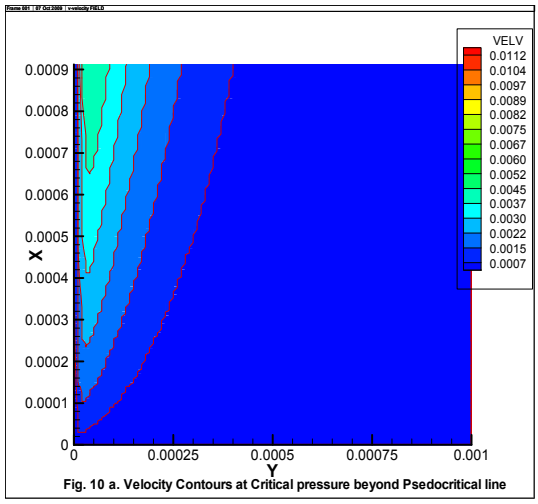

Fig. 10 a. Velocity Contours at Critical pressure beyond Psedocritical line

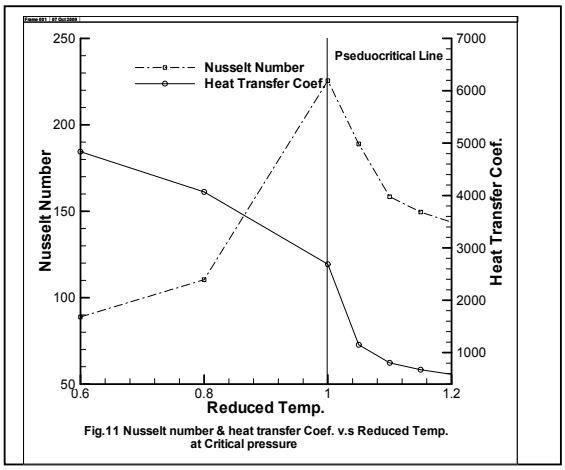

Fig.11 Nusselt number & heat transfer Coef. v.s Reduced Temp. at Critical pressure

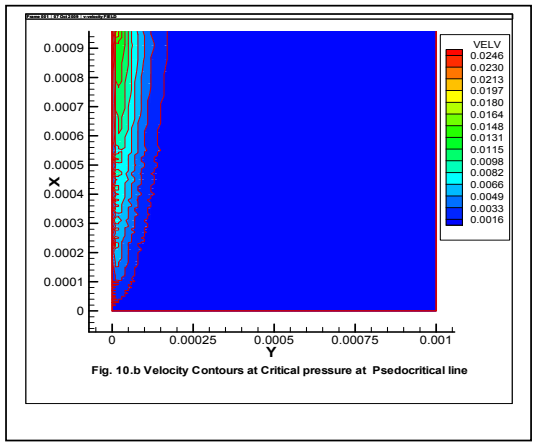

Fig. 10.b Velocity Contours at Critical pressure at Psedocritical line

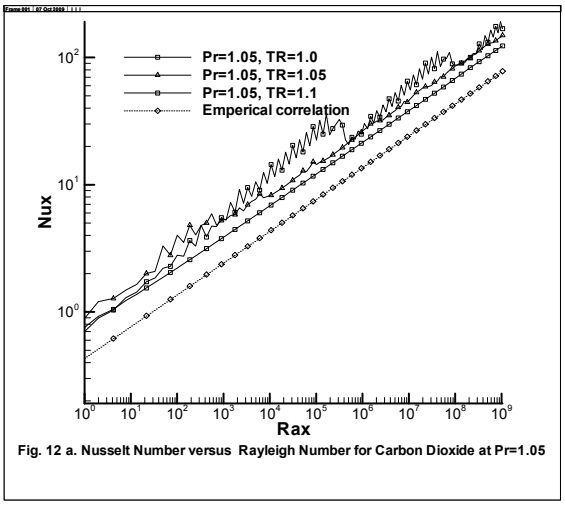

Fig. 12 a. Nusselt Number versus Rayleigh Number for Carbon Dioxide at Pr=1.05

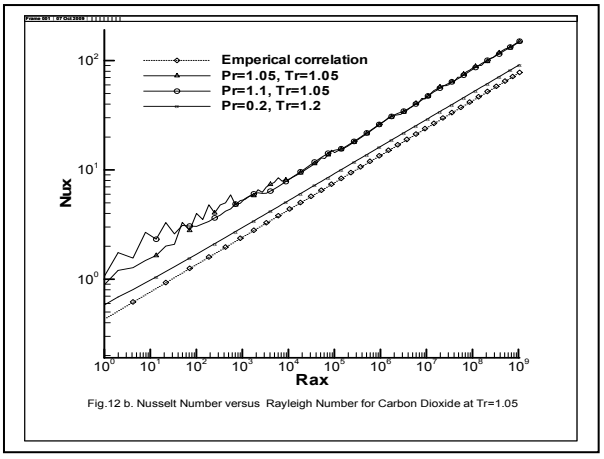

Fig.12 b. Nusselt Number versus Rayleigh Number for Carbon Dioxide at Tr=1.05